Chemosphere 302 (2022) 134770

Contents lists available at ScienceDirect

Chemosphere

journal homepage: www.elsevier.com/locate/chemosphere

# Effects of organic sulfur and arsenite/dissolved organic matter ratios on arsenite complexation with dissolved organic matter

Lena Abu-Ali, Hyun Yoon, Matthew C. Reid *

*School of Civil & Environmental Engineering, Cornell University, Ithaca, NY, USA*

## HIGHLIGHTS

- 20–60% of As(III) can bind to DOM at environmentally-relevant As/DOC ratios.
- Higher organic sulfur content in DOM leads to greater complexation with As (III).
- "Strong" binding site densities are related to organic sulfur concentrations.
- As(III) uptake into bacterial cells is inhibited in the presence of S-rich DOM.

## GRAPHICAL ABSTRACT

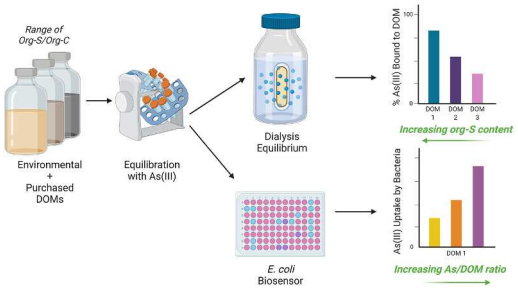


## ARTICLE INFO

Handling Editor: X. Cao

## ABSTRACT

The speciation and fate of arsenic (As) in soil-water systems is a topic of great interest, in part due to growing awareness of As uptake into rice as an important human exposure pathway to As. Rice paddy and other wetland soils are rich in dissolved organic matter (DOM), leading to As/DOM ratios that are typically lower than those in groundwater aquifers or that have been used in many laboratory studies of As-DOM interactions. In this contribution, we evaluate arsenite (As(III)) binding to seven different DOM samples at As/DOM ratios relevant for wetland pore waters, and explore the chemical properties of the DOM samples associated with high levels of As(III)-DOM complexation. We integrate data from wet chemical analysis of DOM chemical properties, dialysis equilibrium experiments, and two-site ligand binding models to show that in some DOM samples, 15–60% of As (III) can be bound to DOM at environmentally-relevant As/DOM ratios of 0.0032–0.016 μmol As/mmol C. Binding decreases as the As(III)/DOM ratio increases. The organic sulfur ($S_{org}$) content of the DOM samples was strongly correlated with levels of As(III)-DOM complexation and "strong" binding site densities, consistent with theories that thiols are strong binding ligands for As(III) in natural organic matter. Finally, a whole-cell *E. coli* biosensor assay was used to show that DOM samples most effective at complexing As(III) also led to decreased microbial As(III) uptake at low As/DOC ratios. This work demonstrates that naturally-occurring variations in the $S_{org}$ content of DOM has a significant impact on As(III) binding to DOM, and has implications for As(III) availability to microorganisms.

* Corresponding author. School of Civil and Environmental Engineering, Cornell University, Ithaca, NY, 14853, USA.
*E-mail address:* mcr239@cornell.edu (M.C. Reid).

https://doi.org/10.1016/j.chemosphere.2022.134770
Received 14 February 2022; Received in revised form 19 April 2022; Accepted 25 April 2022
Available online 29 April 2022

## 1. Introduction

Arsenic (As) is an environmental contaminant and human carcinogen of global importance (Jomova et al., 2011; Smedley and Kinniburgh, 2002). There is growing interest in the speciation and fate of As in rice paddy soils, since rice consumption is an important pathway for human exposure to As (Li et al., 2011; Zhao et al., 2009). The biogeochemical processes regulating the mobilization of As from mineral surfaces in anaerobic subsurface environments are relatively well-understood (Fendorf et al., 2010), but many of the biogeochemical controls on As speciation in reducing pore waters are less well understood. There are notable knowledge gaps around methylation-demethylation reactions (Reid et al., 2017; Chen et al., 2019; Viacava et al., 2022), formation of thioarsenic species (Wang et al., 2020), and As complexation with dissolved organic matter (DOM) (Buschmann et al., 2006; Ren et al., 2017; Hoffmann et al., 2012). The role of DOM may be particularly important in rice paddies and other wetland environments because, in contrast to many surface and groundwaters, these systems are rich in DOM, with dissolved organic carbon (DOC) concentrations frequently exceeding 100 mg C/L (Aftabtalab et al., 2022; Maguffin et al., 2020).

There is a lack of consensus around binding mechanisms between As and DOM, particularly for trivalent arsenite (As(III)) that is considered the predominant inorganic As species in reducing systems. Arsenate (As (V)) is anionic at environmentally relevant pH, and is known to form ternary complexes with DOM through cation bridging reactions with Ca or Fe(III) species (Aftabtalab et al., 2022; Mikutta and Kretzschmar, 2011; Lenoble et al., 2015; Yao et al., 2020; Sharma et al., 2010; Bauer and Blodau, 2009). Cation bridging mechanisms have also been shown to influence DOM complexation of As(III) (Liu et al., 2011), which is neutral in most wetland pore waters, but cation bridging is thought to be less significant for As(III) than with As(V) (Warwick et al., 2005). Modeling of As(III)-DOM complexation data indicates the presence of both “strong” and “weak” binding sites for As(III) in humic acids (Liu and Cai, 2013; Fakour and Lin, 2014), though the identity of the “strong” binding sites has been disputed. Buschmann et al. (2006) and Lenoble et al. (2015) postulate a role for ligand exchange reactions between As(III) and oxygen-containing functionalities (e.g., carboxylate and phenolic moieties), and there is spectroscopic evidence for these ligand exchange reactions with a peat natural organic matter (Hoffmann et al., 2013; Eberle et al., 2020). Thiol functional groups (R–SH) have also recently been shown to act as important binding sites controlling As (III) complexation with natural organic matter (Hoffmann et al., 2012; Eberle et al., 2020; Catrouillet et al., 2015; Langner et al., 2012, 2013). As(III), like other “soft” metal(loid)s, has a high affinity for reduced organic sulfur ($S_{org}$) moieties and is known to bind to thiol groups in proteins, to model thiol compounds like glutathione (Spuches et al., 2005), and thiol functionalities in phytochelatins, which is how plants sequester As(III) in roots and stems (Song et al., 2010). Many questions remain regarding the role of DOM-associated thiols in mediating aqueous complexation reactions between As(III) and DOM, including conditional stability constants and implications for As bioavailability. Arsenic uptake into bacterial cells is a prerequisite for many microbe-mediated transformations of As like methylation-demethylation reactions and production of volatile arsines (Slyemi and Bonnefoy, 2012; Zhang and Reid, 2022), so effects of extracellular water chemistry on As(III) bioavailability may be an important control on As biotransformation and fate in the environment (Zhu et al., 2014).

The significance of As(III) binding to DOM in environmental waters is also unclear. Early work on this topic has shown that the fraction of As (III) bound to DOM will depend on both the As/DOC ratio and the composition of the DOM (Buschmann et al., 2006; Redman et al., 2002), both of which vary widely in the environment. A number of studies have used laboratory experiments with purified humic acids (HAs) to conclude that As(III) binding to DOM is of minor importance at the As/DOC ratios examined in their studies (Buschmann et al., 2006; Liu and Cai, 2010). However, other studies employing freshly-collected environmental DOM samples have concluded that a significant fraction of As(III) can be bound to DOM (Lin et al., 2017). For example, in a groundwater sample with an As/DOC ratio of 1.2 μmol As/mmol C more than 50% of the As was determined to be complexed with DOM (Redman et al., 2002). A recent review of As-DOM interactions in soils (Aftabtalab et al., 2022) shows that an As/DOC ratio of 1.2 μmol As/mmol C is relatively high for soil-water systems, with roughly half of the surveyed samples characterized by As/DOC ratios <0.1 μmol As/mmol C, presumably leading to greater levels of complexation (Table S1). As/DOC ratios observed in a recent study of Arkansas rice paddy pore waters were also lower than values used in many prior laboratory studies, with a median and mean As/DOC ratio of 0.017 and 0.041 μmol As/mmol C, respectively (Figure S1) (Maguffin et al., 2020).

The objectives of this study are: (1) Quantify As(III) binding to DOM with different compositions, using As/DOC ratios that are relevant for rice paddies and other DOM-rich soil-water environments; (2) Evaluate the role of the $S_{org}$ content of DOM in As(III) binding to DOM; and (3) Determine the impacts of DOM-As(III) complexation on As bioavailability, using a whole-cell biosensor fluorescence method (Pothier et al., 2018). We focused on As(III) because it is thought to be the dominant inorganic As species in reducing environments, and because mechanisms for As(III)-DOM binding are not clear. We hypothesized that the $S_{org}$ content of the DOM will be associated with higher As(III)-DOM binding, particularly at low As/DOC ratios, due to the role of thiol ligands as binding sites for As(III). Greater As(III)-DOM complexation was also expected to decrease microbial uptake, since As bound to DOM molecules is thought to be less bioavailable for uptake through membrane transport channels (Pothier et al., 2020).

## 2. Materials and methods

### 2.1. DOM preparation

Suwannee River Humic Acid III (SRHA), Upper Mississippi River Natural Organic Matter (MNOM), and Suwannee River Natural Organic Matter (SRNOM) were purchased from the International Humic Substances Society (IHSS). MNOM and SRNOM were isolated using reverse osmosis, while SRHA was isolated using solid-phase extraction with an XAD-8 resin that adsorbs hydrophobic fractions of the aqueous sample. IHSS materials were dissolved in anoxic Milli-Q water to achieve a final concentration of at least 200 mg C/L. The solution was then vacuum-filtered using a sterile 0.22 μm membrane filter (Corning), wrapped in aluminum foil, and stored in a gas-tight container at 4 °C.

DOM was also extracted from soils and other environmental media. Arkansas soil was collected from the upper 20 cm of rice paddy soil from the Dale Bumpers National Rice Research Center in Stuttgart, AR. This soil was air-dried prior to DOM extraction. Beebe Lake sediment was collected from the upper 20 cm of the shallow shores of Beebe Lake in Ithaca, NY, and immediately transferred to heat-sealed $N_2$-filled mylar bags. Sapsucker Woods (SW-1) soil was collected from a *Typha latifolia* dominated wetland in Ithaca, NY, and immediately transferred to a heat-sealed $N_2$-filled mylar bag. Pine needles and woodchips (PW) were collected from pine trees in Central NY. Solid material was mixed with a 0.05 M KCl solution at a solid:liquid mass ratio of 1:2 and agitated in a gas-tight container on an orbital shaker for 48 h with periodic sonication. The slurry was vacuum filtered using a sterile 0.22 μm membrane filter (Corning) inside an anaerobic chamber. Filtered solutions were stored in gas-tight containers at 4 °C until use. All DOM preparation was performed inside a Coy anaerobic chamber with <10 ppm $O_2$ to protect the speciation of the functional groups within the DOM as well as the As (III).

### 2.2. Chemical characterization of DOM samples

Dissolved organic carbon was measured via the NPOC method with a Shimadzu TOC-L analyzer. Total sulfur ($S_{Tot}$) was measured via an Agilent 8900 Triple Quadrupole ICP-MS. The anionic inorganic sulfur (S) species sulfate, sulfite, and thiosulfate were analyzed via anion exchange chromatography, while $Ca^{2+}$ was measured using cation exchange chromatography (Dionex ICS-2100). Sulfide was determined using the Cline method. 4 mL of filtered anoxic sample was preserved by addition of 1 mL of 0.05 M zinc acetate. A 1 mL aliquot of this preserved sample was added to 80 μL of Cline reagent (*N*,*N*-dimethyl-*p*-phenylenediamine sulfate, $FeCl_3 \bullet 6H_2O$, in 50% HCl), shaken, and incubated for 30 min in the dark. The absorbance at 664 nm was measured and compared to an $Na_2S$ calibration curve for sulfide determination. To quantify the potential presence of elemental sulfur or polysulfides, the Cline method was performed before and after reducing samples with dithiothreitol (DTT) (Kwasniewski et al., 2011). The molar $S_{org}$ to DOC ratios in the IHSS samples and environmental extracts were then determined as the difference between $S_{Tot}$ and the sum of the inorganic S species, normalized by the DOC concentration:

$$\frac{[S_{org}]}{[DOC]} = \frac{[S_{Tot}] - \left([SO_4^{2-}] + [SO_3^{-}] + 2[S_2O_3^{2-}] + [S^{2-}]\right)}{[DOC]} \quad (1)$$

### 2.3. Quantities in brackets represent molar concentrations

The ferrozine method was used for determination of Fe(II) (Stookey, 1970). Samples for minor and trace element analysis (As, Al, Fe, Zn) were preserved in 2% trace metal grade nitric acid and measured via ICP-MS (Agilent 7800) with a helium reaction cell and rhodium as an in-line internal standard. Potential polyatomic interference from ArCl at $m/z = 75$ was assessed by testing samples diluted in 2% trace metal grade HCl, and none was detected. Calibration standards were prepared using a traceable multi-element standard.

### 2.4. Dialysis equilibrium experiments

Dialysis equilibrium experiments were used to quantify the binding of As(III) to DOM. All steps of the dialysis experiments were performed inside an anaerobic chamber. A 7 mL solution of As(III) and DOM at three different As/DOC ratios (0.0032, 0.016, 0.16 μmol As/mmol C; fixed DOC with varying As) were pre-equilibrated inside aluminum foil-wrapped centrifuge tubes for 24 h by mixing on a tube rotator. After this pre-equilibration period, a 2 mL aliquot of the solution was collected for initial characterization of the As(III)-DOM solution. The remaining 5 mL of the As(III)-DOM solution were then transferred to a Float-A-Lyzer dialysis device (Spectra-Por) with a pore size of 0.1–0.5 kDa. The smallest available pore size range was selected to ensure that As bound to low molecular weight organic molecules would be retained inside the tubing, while unbound As(III) could diffuse through the membrane. The dialysis tubing was placed in 500 mL of As-free bulk solution (0.05 M KCl, 0.15 mM sodium azide, 1 mM bicarbonate buffer, pH 7) in 500 mL opaque HDPE containers at a room temperature of 22 °C. Preliminary experiments showed no sorption of As or DOC to HDPE containers, stir bars, or dialysis devices. Dialysis devices were found to leach significant amounts of DOC; this was remedied by soaking devices in 20% ethanol for at least 24 h before experiments and rinsing thoroughly with DI water. The bulk solution and dialysis devices were stirred on a magnetic plate for 48 h to allow for diffusion of unbound As across the membrane. At the end of the equilibration time, solutions inside and outside the dialysis tubing device were sampled, filtered through 0.22 μm syringe membrane filters, and analyzed for As via ICP-MS.

Concentrations of bound and free As were determined by performing a mass balance on As in the dialysis tubing at t = 0 and t = 48 h, since free As concentrations in the bulk solution were sometimes below the limit of quantification. Free As concentrations in the bulk solution at t = 48 h, $C_{bulk,t\ =\ 48}$, were estimated using the equation:

$$C_{bulk,t=48} = \frac{C_{tubing,t=0}V_{tubing} - C_{tubing,t=48}V_{tubing}}{V_{bulk}} \quad (2)$$

where $C_{tubing,t\ =\ 0}$ and $C_{tubing,t\ =\ 48}$ are the As concentration measured in the dialysis tubing at t = 0 and t = 48, respectively [mol $L^{-1}$], $V_{tubing}$ is the volume of solution inside the dialysis tubing (5 mL), and $V_{bulk}$ is the bulk solution volume (500 mL). The percentage of As bound to DOM was then determined using the equation:

$$\%bound = \frac{\left(C_{tubing,t=48} - C_{bulk,t=48}\right)V_{tubing}}{\left(C_{tubing,t=0}V_{tubing,t=0}\right)} \times 100 \quad (3)$$

Note that in this calculation the system boundaries are defined as the dialysis tubing and bulk solution, so As bound to DOM is expressed as a percentage of the total As in the system, inclusive of the dialysis tubing and the bulk solution.

### 2.5. Scatchard plot analysis

Concentrations of free and bound As determined from dialysis equilibrium experiments were used in a graphical Scatchard plot analysis to estimate binding site densities and conditional stability constants for a subset of DOM samples (Liu and Cai, 2010, 2013). The general equation for the Scatchard equation with *i* binding sites is (Brezonik and Arnold, 2011; Attie and Raines, 1995):

$$[As]_{bound} = \sum_{i=1}^{n} \frac{B_{max,i}[As]_{free}}{\frac{1}{K_{s,i}} + [As]_{free}} \quad (4)$$

$[As]_{bound}$ and $[As]_{free}$ are the bound and free As concentrations [mol $L^{-1}$], respectively, $B_{max,i}$ is the total concentration of binding site *i* [mol $L^{-1}$], and $K_{s,i}$ is the conditional stability constant for binding site *i* [L $mol^{-1}$]. Previous modeling of As(III) binding to heterogeneous DOM using Scatchard analysis has shown that DOM can be simplified as having n = 2 independent binding sites, a "strong" and "weak" binding site (Liu and Cai, 2013). For the case of n = 2, eqn. (4) has four parameters: $B_{max,ss}$, $B_{max,ws}$, $K_{s,ss}$, and $K_{s,ws}$, where the ss and ws subscripts refer to strong and weak sites, respectively. To estimate these parameters, $[As]_{bound}/[As]_{free}$ is plotted against $[As]_{bound}$. Methods for estimating the parameters from this graphical approach are described in Brezonik and Arnold (2011) and are illustrated in Figure S2.

### 2.6. E. coli biosensor assay

A whole cell fluorescent biosensor method (Pothier et al., 2018; Stocker et al., 2003) was used to determine the microbial uptake of As (III) in the presence of select DOM samples. The principle for the biosensor is that binding of intracellular As(III) to the ArsR As (III)-responsive transcriptional repressor allows for the expression of the fluorescent *mCherry* gene (Stocker et al., 2003), leading to greater fluorescence when intracellular As concentrations are greater. The construction and implementation of this biosensor has been described previously (Pothier et al., 2018, 2020). The biosensor was thawed and plated onto an LB plate containing 120 μg/mL ampicillin, which was incubated overnight at 37 °C. Experiments were performed with biological quadruplicates, with four independent colonies inoculated into different autoclaved narrow mouthed Pyrex® 125-mL flasks containing 100 mL of growth media at pH 7. A complete description of the growth media is available in supporting information (SI). Culture flasks were incubated on an orbital shaker at 37 °C at 200 rpm until OD600 reached ~1.0.

For the As(III) exposure experiments, As(III) was pre-incubated with MNOM and SRHA for 2–3 h inside an anaerobic chamber at the same As (III)/DOC ratios tested in the dialysis equilibrium experiment: 0.0032, 0.016, 0.16 μmol As/mmol C. Unlike the dialysis experiments, it was necessary to fix the As(III) concentration since the biosensor response is

highly sensitive to As(III) concentrations, so in order to evaluate differences across different As/DOC ratios it was necessary to maintain a constant As concentration. The biosensor was then exposed to the As (III)-DOM solution and fluorescence intensities (RFU) and optical density at 600 nm (OD600) were measured with an Infinite 200 fluorescence plate reader (Tecan, Research Triangle Park, NC) for 20 h. The excitation wavelength was 560 nm and fluorescence was measured at 620 nm. Endpoint fluorescence normalized by OD600 at 20 h was used to evaluate differences between microbial uptake of As across different DOM samples and As/DOC ratios. A one-way ANOVA with a Tukey's post hoc test using R (RCore, 2013) were used to assess data, and differences between assays of different conditions were considered significant when $p < 0.05$.

## 3. Results

### 3.1. DOM characterization

A summary of the composition of the DOM samples examined in this study is in Table 1. Because $SO_4^{2-}$ was detected in the IHSS samples, the $S_{org}$/DOC reported for these samples differs somewhat from the elemental ratios reported for these samples by IHSS. Molar $S_{org}$/DOC ratios ranged from $9.6 \times 10^{-4}$ for SRHA to $6.38 \times 10^{-3}$ for MNOM. Fe and Al, which may play a role in ternary complexation reactions, ranged from $1.5 \times 10^{-4}$ to $1.6 \times 10^{-2}$ mmol Fe/mmol C and $1.3 \times 10^{-5}$ to $1.14 \times 10^{-3}$ mmol Al/mmol C, respectively. SW-1, which was extracted from a reducing wetland soil, had a particularly high Fe concentration. 12% of the total Fe was determined to be Fe(II) using the ferrozine assay, indicating that most of the Fe was Fe(III) complexed with DOM or in colloidal Fe(III) oxyhydroxide phases. None of the samples contained sulfide above the lower limit of quantification (1 μM) and the DTT reduction method showed no evidence of elemental sulfur or polysulfides in any sample. All DOMs had negligible As concentrations.

### 3.2. As(III)-DOM binding in dialysis equilibrium experiments

The percentage of As bound to DOM was determined using Equation (3). The percentage of bound As ranged from close to 0 to more than 60 percent, with mostly good agreement between duplicates. With the exception of SW-1, all DOMs showed decreasing binding with increasing As/DOC ratio (Fig. 1), in agreement with previous studies (Buschmann et al., 2006; Liu and Cai, 2010) and a conceptual model in which binding is controlled by a finite number of binding sites. Among the IHSS samples, MNOM had the highest binding, with roughly 62% of the As bound at the 0.0032 μmol As/mmol C ratio, followed by SRNOM and SRHA. Roughly 18% of the As was bound to SRHA at the 0.0032 μmol As/mmol C ratio. The percentage of As bound by the Arkansas, Beebe Lake, and PW DOMs was between 25% and 35% at the 0.0032 μmol As/mmol C ratio. At the highest As/DOC ratio of 0.16 μmol As/mmol C, the percentage binding had decreased to <10% for all DOMs except SW-1. MNOM also had the highest percentage of bound As at this ratio, with 6% of the As bound. The SW-1 DOM stands out as the only DOM to show only a slight decrease in binding from the 0.0032–0.16 μmol As/mmol C ratio, and a relatively high percentage of As bound (55%) at the highest As/DOC ratio.

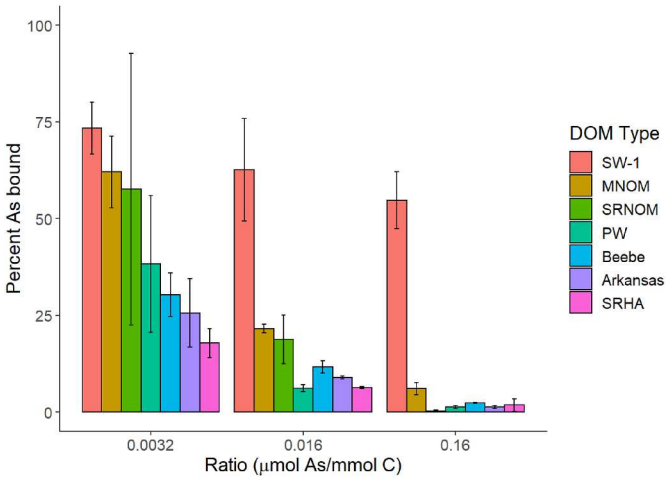


**Fig. 1.** The percentage of As(III) bound to different DOM samples at three different As/DOC ratios. Bars show the mean of duplicate experiments and error bars show the range of the duplicates.

### 3.3. Relationships between As(III)-DOM binding and DOM characteristics

A correlation matrix of the DOM chemical properties with the percentage of bound As showed that the $S_{org}$/DOC ratio was significantly correlated with As-DOM binding ($p < 0.001$) (Fig. 2). MNOM has the highest $S_{org}$/DOC ratio and the second highest level of As binding across all As/DOC ratios, behind the Fe(III)-rich SW-1. SRHA, Beebe Lake, and Arkansas DOMs have the lowest $S_{org}$/DOC ratios and consistently show the lowest levels of bound As. While SW-1 had a high Fe/DOC ratio and a high level of binding across all three As/DOC ratios, there was no relationship between As-DOM binding and the Fe/DOC ratio with the other DOMs.

Further exploration of the data with a principal component analysis (PCA) biplot reveals similar relationships between DOM chemical characteristics and As binding percentages (Figure S3). SW-1 was excluded from the PCA analysis. The percentage of As bound is strongly correlated with the $S_{org}$/DOC ratio. MNOM, SRNOM, and PW, the three DOM samples with the greatest level of As binding besides SW-1, cluster together in the southeast quadrant. Concentrations of cationic elements (i.e., molar ratios of Fe, Al, Ca, Mg, and Zn to DOC) were not correlated

**Table 1**
Summary of DOM Chemical Properties.

| DOM | Source | DOC (mmol C/L) | $S_{Tot}$/C (mmol S/mmol C) | $S_{Tot}$/C from IHSS† (mmol S/mmol C) | $S_{org}$/C◇ (mmol S/mmol C) | Fe/C (mmol Fe/mmol C) | Al/C (mmol Al/mmol C) |
|---|---|---|---|---|---|---|---|
| SRHA | IHSS | 31.3 | $1.44 \times 10^{-3}$ | $3.78 \times 10^{-3}$ | $9.60 \times 10^{-4}$ | $7.84 \times 10^{-4}$ | $1.14 \times 10^{-3}$ |
| MNOM | IHSS | 20.8 | $2.17 \times 10^{-2}$ | $1.97 \times 10^{-2}$ | $6.38 \times 10^{-3}$ | $3.42 \times 10^{-4}$ | $1.44 \times 10^{-4}$ |
| SRNOM | IHSS | 18.3 | $1.46 \times 10^{-2}$ | $1.32 \times 10^{-2}$ | $2.56 \times 10^{-3}$ | $6.90 \times 10^{-4}$ | $8.27 \times 10^{-4}$ |
| Arkansas | Environmental extract | 5.0 | $2.70 \times 10^{-2}$ | NA | $4.00 \times 10^{-4}$ | $1.72 \times 10^{-4}$ | $1.28 \times 10^{-4}$ |
| Beebe | Environmental extract | 17.9 | $3.35 \times 10^{-4}$ | NA | $3.35 \times 10^{-4}$ | $1.03 \times 10^{-3}$ | $1.32 \times 10^{-5}$ |
| PW | Environmental extract | 58.3 | $8.13 \times 10^{-3}$ | NA | $3.72 \times 10^{-3}$ | $1.51 \times 10^{-4}$ | $2.71 \times 10^{-4}$ |
| SW-1 | Environmental extract | 15.0 | $1.07 \times 10^{-3}$ | NA | $1.07 \times 10^{-3}$ | $1.59 \times 10^{-2}$ | $7.92 \times 10^{-5}$ |

NA = Not Applicable; †Based on Elemental Concentrations reported by IHSS; ◇Determined using Eqn. (4). Additional information on the chemical properties of SRHA, MNOM, and SRNOM are available from IHSS.

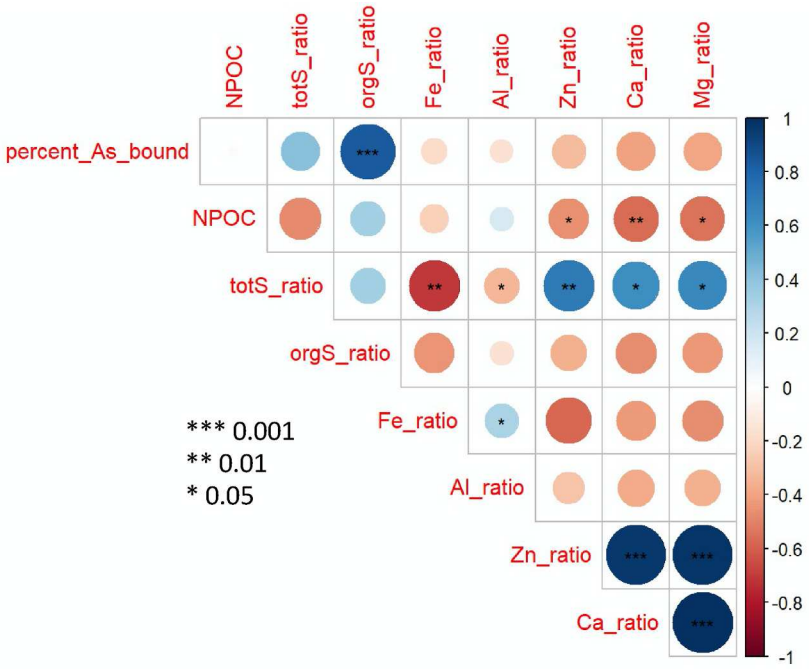


**Fig. 2.** Correlation matrix of macroscopic chemical properties of DOM samples with the percentage of As (III) bound to DOM samples. Ratios refer to the ratio of the analyte concentration to the DOC concentration (e.g., "orgS_ratio" is $S_{org}$/DOC). The color bar shows the Pearson correlation coefficient, the area of the circle represents the absolute value of the corresponding correlation coefficient, and the significance level is indicated by the number of asterisks. (For interpretation of the references to color in this figure legend, the reader is referred to the Web version of this article.)

with As binding levels. This is notable since cationic species of Ca and Fe have been linked to DOM complexation with As(V) (Lenoble et al., 2015) and, to a somewhat lesser extent, As(III) (Hoffmann et al., 2013), but here there was no evidence for these cationic species having a large impact on As(III)-DOM binding.

### 3.4. Scatchard analysis

Based on the finding of a relationship between $S_{org}$/DOC ratios and As(III)-DOM binding, we performed further chemical and biological analysis on MNOM and SRHA to further explore the binding sites responsible for As(III) complexation. These two DOM samples were selected because they exhibited significantly different binding of As(III) (Fig. 1) and represent a high and low $S_{org}$/DOC ratio (Table 1). Additional dialysis equilibrium experiments were performed with these two DOM samples to gather more data. Scatchard plots and estimated model parameters for these two DOM samples are shown in Fig. 3. Nonlinearity in Scatchard plots indicated the presence of both "strong" and "weak" binding sites, as has been shown previously with DOM from other sources (Liu et al., 2011; Fakour and Lin, 2014). The "strong" binding site densities of the MNOM and SRHA were estimated to be 0.018 ± 0.007 and 0.0048 ± 0.0024 μmol/mmol C, respectively. The strong site density in MNOM was 3.8 times higher than the strong site density in SRHA. The conditional stability constants estimated for the two DOM samples were similar, with log $K_{ss}$ = 2.42 for MNOM and log $K_{ss}$ = 2.33 for SRHA, suggesting that the binding mechanism for both DOM samples may be similar.

### 3.5. Biosensor assay of As bioavailability

The biosensor assay was used to evaluate the effects of MNOM and SRHA on As(III) bioavailability across the range of As/DOC ratios tested in the dialysis equilibrium experiments. Biosensor fluorescence normalized by microbial biomass at the endpoint of the 20 h growth assay, a measure of As uptake (Pothier et al., 2018), is shown in Fig. 4. For both MNOM and SRHA, there was a significant decrease in microbial

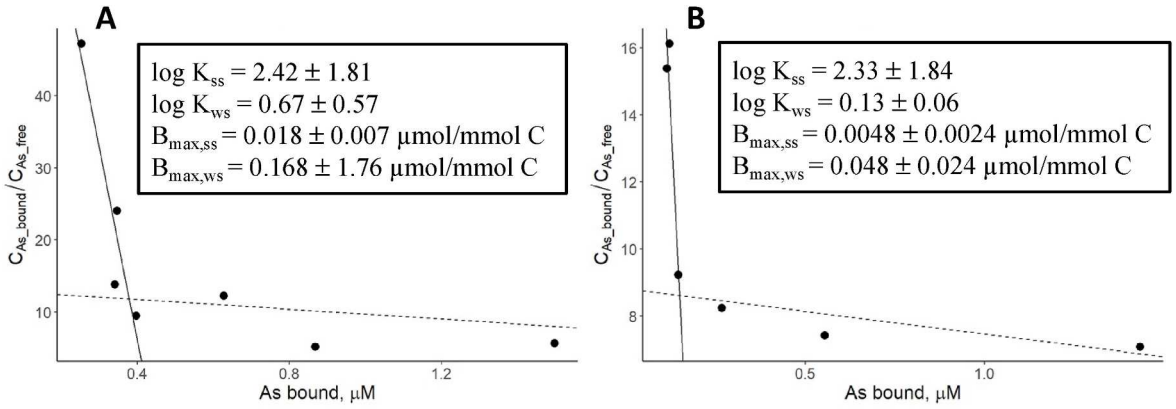


**Fig. 3.** Scatchard plot analysis of As(III) binding with (A) MNOM and (B) SRHA, indicating the existence of "strong" and "weak" binding sites. The x-axis represents the concentration of As bound to DOM in μM. The y-axis represents the dimensionless ratio of DOM-bound As to free, uncomplexed As. $K_{ss}$ and $K_{ws}$ are the conditional stability constants for the strong and weak sites, respectively, and $B_{max,ss}$ and $B_{max,ws}$ are the maximum binding site densities for the strong and weak sites, respectively. Data come from dialysis equilibrium experiments with an MNOM concentration of 20.8 mmol C/L and SRHA concentration of 31.3 mmol C/L (Table 1). Model fits are based on linear least-squares regression. See Figure S2 for details on data interpretation.

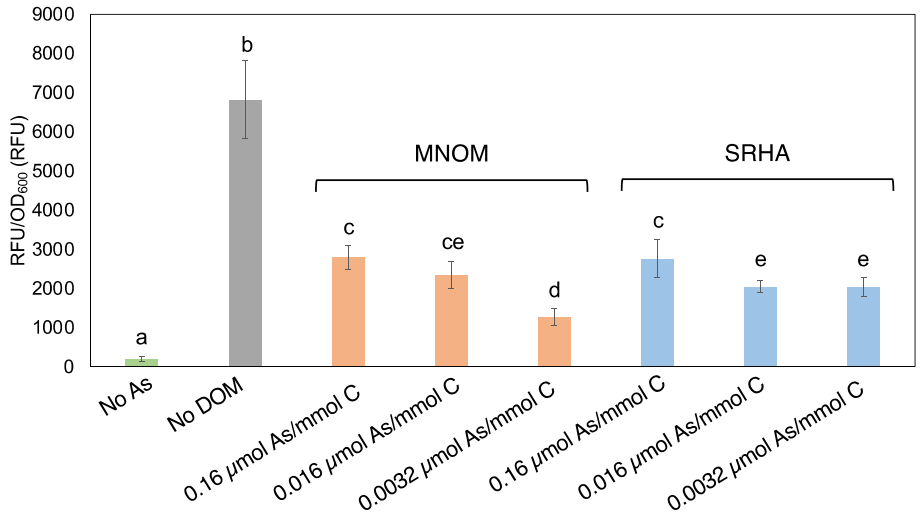


**Fig. 4.** Biosensor fluorescence (RFU) at t = 20 h normalized by $OD_{600}$, a measure of microbial biomass. The $RFU/OD_{600}$ ratio is a measure of microbial As uptake normalized by microbial biomass. Bars show mean values and error bars show standard deviations of n = 4 replicates. Letters refer to statistically significant differences in means between groups.

uptake as the As/DOC ratio decreased, consistent with the expectation that greater As-DOM binding at low As/DOC ratios would lead to a decrease in bioavailability. For MNOM, fluorescence decreased by 54% from the 0.16 to the 0.0032 μmol As/mmol C ratio, while for SRHA the decrease was just 26%. At the 0.0032 μmol As/mmol C, fluorescence was 37% lower in the presence of MNOM compared to measurements in the presence of SRHA. These significant differences in biosensor fluorescence between MNOM and SRHA are consistent with the patterns seen in As(III)-DOM binding from dialysis equilibrium experiments, where As (III) bound to MNOM to a much greater extent than it did SRHA.

Notably, all of the experiments with DOM, including those at the highest As/DOC ratio, exhibited significantly lower fluorescence than the No DOM control. This may be due in part to inhibited As uptake even at these high ratios, but it may also be caused by a catabolite repression mechanism in which the presence of labile carbon in the DOM pools leads to a decrease in uptake sites (Pothier et al., 2018).

## 4. Discussion

### 4.1. As(III) binding to DOM: effects of As/DOC ratios

The fraction of As(III) bound to DOM depended on both the As/DOC ratio and DOM chemical properties. Our results indicate that a significant fraction of As(III) can be bound to DOM at the environmentally-relevant ratios examined here, with roughly 20–60% of the As(III) bound to DOM at the 0.0032 μmol As/mmol C ratio and >15% bound for some DOM samples at the intermediate 0.016 μmol As/mmol C ratio (Fig. 1). While <5% of the As(III) was bound for most DOM samples at the 0.16 μmol As/mmol C ratio, it is common for environmental soil-water systems to be characterized by As/DOC ratios below this level (Table S1).

Arsenic/DOC ratios in a rice paddy soil with a moderately high As concentration of 19.7 mg/kg (Maguffin et al., 2020) were recently shown to have a median As/DOC ratio of 0.017 μmol As/mmol C (Figure S1), similar to the intermediate value tested in dialysis equilibrium experiments. Roughly 20% of the As(III) was DOM-bound for the MNOM and SRNOM DOM samples at this ratio. A recent review of 16 studies on As-DOM interactions in the soil solution found that five studies reported As/DOC ratios <0.007 μmol As/mmol C (Table S1) (Aftabtalab et al., 2022), a range where our data showed that bound As was an important component of the total As pool (Fig. 1). Half of the studies in the review had As/DOC ratios >0.16 μmol As/mmol C, where our results suggest that As(III) binding to DOM would be of minor importance. This analysis of environmentally-relevant As/DOC ratios shows that wetland environments with low As/DOC ratios, and consequently the potential for high levels of As(III)-DOM binding, are not uncommon. DOM-bound As(III) is largely unrecognized in geochemical As speciation models, and our results suggest that it could represent an important portion of the total As pool, particularly in systems where As/DOC ratios are less than roughly 0.02 μmol As/mmol C. This is most likely to occur in systems with high levels of DOM and low-to-moderate levels of soil As. We acknowledge that in soils with very high levels of As (e.g., paddy soils in Bangladesh irrigated with groundwater with high As levels (Roberts et al., 2011)), this condition is unlikely to be met.

### 4.2. As(III) binding to DOM: effects of organic sulfur

The $S_{org}$ density of DOM samples was strongly correlated with As binding (Fig. 2). This supports the hypothesis that S-containing ligands, like thiols, in DOM serve as key binding sites for As(III). The result is consistent with findings reported in Hoffmann et al. (2012) that As(III) "sorption" to a bisulfide-reacted HA was correlated with the S content of the HA. In our study, the $S_{org}$/DOC ratio was 6.7 times higher in MNOM than in SRHA, while the "strong" binding site density estimated from Scatchard-plot analysis was only 3.8 times higher. This discrepancy between the $S_{org}$ and "strong" site ratios may be due in part to experimental error, given the relatively large uncertainties in the Scatchard-derived parameters (Fig. 3). The discrepancy may also be due to thiols representing a different fraction of the $S_{org}$ in MNOM compared to SRHA, an observation that has been shown in prior surveys of thiol/$S_{org}$ ratios in aquatic organic matter (Skyllberg et al., 2005).

There has been no clear consensus regarding the mechanisms for As (III) binding by DOM, and until recently many studies of As(III)-DOM interactions did not report the $S_{org}$ content of the DOM samples studied (Liu and Cai, 2010, 2013; Redman et al., 2002; Lin et al., 2017). Buschmann et al. (2006) described a range of potential mechanisms involving oxygen-containing functional groups in DOM, while modeling in Lenoble et al. (2015) assumed that the active binding sites in SRHA were carboxylic and phenolic sites. More recent studies have directed more focus on the role of $S_{org}$ ligands. Reacting HAs with bisulfide has been shown to increase both the S content of the HA and As(III)-HA complexation (Hoffmann et al., 2012; Catrouillet et al., 2015). This finding is thought to be due to the incorporation of thiol functionalities in HA by the bisulfide reaction. More recent studies have shown that thiol-modified HAs increase the leaching of As from mining-impacted soils, presumably due to complexation between thiol functionalities

and As (Qian et al., 2022; Xu et al., 2020). The results of the present study extend these prior findings to show that naturally-occurring variations in the $S_{org}$ content of DOM are also associated with differences in the extent of DOM complexation with As(III). We caution that our data do not provide definitive evidence of thiols as the binding site for As(III), but rather show that DOM samples with higher $S_{org}$ content were associated with higher levels of As(III) complexation.

The Fe-rich SW-1 DOM sample exhibited only a small change in As binding percentages across the As/DOC ratios (Fig. 1). This observation suggests a different binding mechanism controlling As speciation, possibly driven by the relatively high Fe(III) content of this sample (Table 1). In their study of As distributions in the presence of both DOM and Fe(III), Bauer and Blodau (2009) showed that when molar Fe/C ratios >0.02, As(V) was primarily associated with colloidal or complexed Fe(III). The molar Fe/C ratio in SW-1 of 0.016 was near the ratio observed in Bauer and Blodau (2009) where As–Fe(III) associations became dominant, while all of the other DOM samples in our study had much lower molar Fe/C ratios $<10^{-3}$. Only a small fraction of the Fe was Fe(II), so it appears that the Fe was primarily colloidal or DOM-complexed Fe(III) that passed through the 0.2 μm membrane used to filter extracts. This Fe(III) could have been present in the in situ soil samples, or it could have been formed during sample collection and/or DOM extraction. This association of As(III) with DOM-complexed and/or colloidal Fe(III) was also shown in Liu et al. (2011), where size exclusion chromatography hyphenated to ICP-MS was used to show that As(III) was associated with Fe in a sample with a molar Fe/C ratio of 0.037. Our results therefore suggest a balance between colloidal/DOM-complexed Fe(III) phases and $S_{org}$ functionalities in controlling As(III) distributions in waters containing both DOM and Fe (III), with molar Fe/DOC ratios ~0.015 and greater associated with strong As(III)–Fe association.

### 4.3. Environmental significance of As(III)-DOM complexation

Binding of As(III) to DOM has traditionally been thought to be of relatively minor environmental importance, especially compared to higher levels of As(V) complexation with DOM (Fakour and Lin, 2014), which is often attributed to cation bridging mechanisms (Hoffmann et al., 2013). In this contribution, we show that DOM-bound As(III) can be a significant part of the total As pool in reducing environments. The discrepancy between earlier studies and the current study is due to both the consideration of As/DOC ratios and the chemical properties of DOM samples. Observations in earlier work of high levels of As(III)-DOM binding at As/DOC ratios as low as 0.003 μmol As/mmol C were not thought to be environmentally-relevant (Buschmann et al., 2006), while recent attention to DOM-rich wetland pore waters suggest that these ratios are common. Another key difference is the choice of DOM sample and its isolation method. Many prior studies on As(III)-DOM interactions used SRHA or Aldrich HA to conclude that As(III)-DOM complexation was minor (Buschmann et al., 2006; Liu and Cai, 2010). We show here that SRHA exhibits the lowest levels of As(III) binding of the seven DOM samples examined, potentially due to its low $S_{org}$ content. In contrast, prior work utilizing environmental DOM isolated without solid-phase extraction showed that >50% of the As(III) was bound to DOM (Redman et al., 2002; Lin et al., 2017). The S content in the hydrophilic fraction of DOM (i.e., the fraction not retained on the moderate hydrophobic XAD-8 resin) is higher than in the humic and fulvic acid fractions (Ma et al., 2001), possibly explaining why the RO-isolated MNOM and SRNOM, which combine HA, FA, and hydrophilic DOM fractions, displayed higher levels of binding to As(III) than SRHA, which is purified using solid-phase extraction. Relatively high dissolved thiol concentrations of 29 μM have been measured in natural waters (Joe-Wong et al., 2012), further suggesting that environmental abundances of thiols may have been traditionally underestimated due to a focus on humic and fulvic acid fractions of DOM.

Geochemical modeling of As(III) complexation with DOM require knowledge of binding site densities and conditional stability constants. The "strong" binding site densities for MNOM and SRHA determined with the Scatchard analysis were small, estimated to be 0.018 and 0.0048 μmol/mmol C, respectively. These binding site densities are similar to values reported in Liu and Cai (2010) for Aldrich HA of 0.0086 μmol/mmol C, but are an order of magnitude lower than values determined for Aldrich HA in Fakour and Lin (2014) of 0.14–0.24 μmol/mmol C. Under the conservative assumption that thiols represent 10% of the $S_{org}$ concentration (Skyllberg et al., 2005) presented in Table 1, the thiol binding site concentrations in these two DOMs is 0.64 and 0.096 μmol/mmol C, respectively. If thiols are indeed the binding site for As(III), this indicates that only ~2–5% of the total thiols were reactive with As(III). This is similar to the observation made in Hoffman et al. (2012) that reduced $S_{org}$ functional groups in Elliot Soil HA were present in very large excess over complexed As(III), and is also consistent with studies of $Hg^{2+}$ binding to NOM that have shown that a very small fraction of reduced $S_{org}$ is available as reactive thiols (Dong et al., 2010). A comparison of the Scatchard-determined site densities and experimental As/DOC ratios shows that at the lowest tested ratio in the dialysis equilibrium experiments (0.0032 μmol As/mmol C), "strong" sites in MNOM were in significant excess of As, while the "strong" sites in SRHA were close to a 1:1 ratio. At the highest ratio (0.16 μmol As/mmol C), strong sites in both MNOM and SRHA were fully saturated, explaining the low level of complexation at this ratio.

Conditional stability constants for binding of As(III) to "strong sites" in DOM reported in the literature are inconsistent. The values reported here for MNOM and SRHA, log $K_{ss}$ = 2.33–2.44, are similar to values reported for As(III) binding to Aldrich humic and fulvic acid in Fakour and Lin (2014) of log $K_{ss}$ = 1.53 to 2.61. In contrast, Liu and Cai (2010) found log $K_{ss}$ to range from 5.9 to 7.0, depending on pH. Neither of these prior studies identified which functional groups the strong sites could be. Catrouillet et al. (2015) estimated log K = 2.9 for 1:1 for monodentate binding between As(III) and thiol functionalities in humic acid. Their explanation for the 1:1 binding stoichiometry is that the large, inflexible structure of humic acid molecules combined with their low thiol density makes it difficult for more than one thiol to bind an As(III) molecule. Spectroscopic studies have found S coordination numbers for As(III) of 1.2 and 1.5 (Hoffmann et al., 2012) in sulfur-reacted humic acid. Our results do not provide direct information on the binding stoichiometry between As(III) and thiol functionalities.

### 4.4. Implications for As bioavailability to microorganisms

The results of the biosensor assay suggest that MNOM is more effective than SRHA at inhibiting the microbial uptake of As(III). This finding is in agreement with the dialysis equilibrium results and Scatchard-plot analysis which showed that the $S_{org}$-rich MNOM had a "strong" binding site density more than three times greater than the site density in $S_{org}$-poor SRHA, leading to a roughly three-fold difference in binding (Fig. 1). Earlier biosensor-based work has demonstrated the effect of lower As/DOC ratios in decreasing microbial uptake of As(III) (Pothier et al., 2020), but our findings are novel in linking decreased bioavailability to the $S_{org}$ content of the DOM sample. Our findings do not provide information on the mechanism for inhibited As uptake, but it is possible that the larger molecular size of DOM-complexed As(III) restricts its uptake through the aquaglyceroporin channels that mediate transport of As(III) and other small, neutral molecules across cellular membranes (Meng et al., 2004; Rosen and Liu, 2009). Inhibition of As (III) uptake driven by formation of As-DOM complexes may impact As biotransformation reactions that depend on the activity of intracellular As metabolism enzymes (e.g., arsenic methylation catalyzed by ArsM enzymes (Reid et al., 2017)), and follow-up research is underway to explore this further.

## 5. Conclusions

The significance and mechanisms of As(III) binding to DOM is not fully understood, and growing concern about As speciation and fate in rice paddies merits new attention to As-DOM interactions in organic-rich environments. Here we show that a significant fraction of As is bound to DOM at As/DOC ratios characteristic of DOM-rich soil-water environments. The $S_{org}$ content of DOM samples with low Fe(III) content was strongly correlated with the fraction of bound As, suggesting that $S_{org}$ moieties like thiols are important binding sites. The Fe(III)-rich environmental extract SW-1 displayed patterns that were distinct from the other DOM samples, suggesting that As(III) association with colloidal or DOM-complexed Fe(III) phases may be more significant than binding to $S_{org}$ functionalities when molar Fe/C ratios are greater than 0.015. While we cannot rule out the possibility that the As(III) in SW-1 may have been oxidized to As(V) during the duration of the dialysis equilibrium experiment, such transformations would be consistent with what would happen in an anaerobic soil environment since samples were prepared and experiments performed in strictly anoxic conditions. Results indicate that DOM-bound As(III) should be considered in As speciation modeling if As/DOC ratios are less than roughly 0.02 μmol As/mmol C, and that complexation modeling based on $S_{org}$ concentrations may be effective as long as the colloidal or DOM-complexed Fe(III) content is relatively low.

## Author statement

**Lena Abu-Ali:** Validation; Methodology; Investigation; Formal analysis; Writing – original draft; Visualization; **Hyun Yoon:** Methodology; Validation; Investigation; Writing – original draft. **Matthew C. Reid:** Conceptualization; Methodology; Formal analysis; Writing – original draft; Writing – review & editing; Funding acquisition; Resources; Supervision; Project administration.

## Declaration of competing interest

The authors declare that they have no known competing financial interests or personal relationships that could have appeared to influence the work reported in this paper.

## Acknowledgments

The authors thank A. Poulain (University of Ottawa) for providing the *E. Coli* biosensor, R. Richardson for the use of a Tecan plate reader, and J. Rohila and A. McClung for providing Arkansas rice paddy soil. Funding was provided by NSF grant 1905175. ICP-MS analysis of total sulfur was carried out at the Dartmouth Trace Element Core Facility, which was established by grants from the National Institute of Health (NIH) and National Institute of Environmental Health Sciences (NIEHS) Superfund Research Program (P42ES007373) and the Norris Cotton Cancer Center at Dartmouth Hitchcock Medical Center.

## Appendix A. Supplementary data

Supplementary data to this article can be found online at https://doi.org/10.1016/j.chemosphere.2022.134770.

## References

Aftabtalab, A., Rinklebe, J., Shaheen, S.M., Niazi, N.K., Moreno-Jiménez, E., Schaller, J., Knorr, K.-H., 2022. Review on the interactions of arsenic, iron (oxy)(hydr) oxides, and dissolved organic matter in soils, sediments, and groundwater in a ternary system. Chemosphere 286, 131790.

Attie, A.D., Raines, R.T., 1995. Analysis of receptor-ligand interactions. J. Chem. Educ. 72 (2), 119.

Bauer, M., Blodau, C., 2009. Arsenic distribution in the dissolved, colloidal and particulate size fraction of experimental solutions rich in dissolved organic matter and ferric iron. Geochem. Cosmochim. Acta 73 (3), 529–542.

Brezonik, P., Arnold, W., 2011. Water Chemistry: an Introduction to the Chemistry of Natural and Engineered Aquatic Systems. OUP USA.

Buschmann, J., Kappeler, A., Lindauer, U., Kistler, D., Berg, M., Sigg, L., 2006. Arsenite and arsenate binding to dissolved humic acids: influence of pH, type of humic acid, and aluminum. Environ. Sci. Technol. 40 (19), 6015–6020.

Catrouillet, C., Davranche, M., Dia, A., Bouhnik-Le Coz, M., Pédrot, M., Marsac, R., Gruau, G., 2015. Thiol groups controls on arsenite binding by organic matter: new experimental and modeling evidence. J. Colloid Interface Sci. 460, 310–320.

Chen, C., Li, L., Huang, K., Zhang, J., Xie, W.-Y., Lu, Y., Dong, X., Zhao, F.-J., 2019. Sulfate-reducing bacteria and methanogens are involved in arsenic methylation and demethylation in paddy soils. ISME J. 13 (10), 2523–2535.

Dong, W., Liang, L., Brooks, S., Southworth, G., Gu, B., 2010. Roles of dissolved organic matter in the speciation of mercury and methylmercury in a contaminated ecosystem in Oak Ridge, Tennessee. Environ. Chem. 7 (1), 94–102.

Eberle, A., Besold, J., Kerl, C.F., Lezama-Pacheco, J.S., Fendorf, S., Planer-Friedrich, B., 2020. Arsenic fate in peat controlled by the pH-dependent role of reduced sulfur. Environ. Sci. Technol. 54 (11), 6682–6692.

Fakour, H., Lin, T.-F., 2014. Experimental determination and modeling of arsenic complexation with humic and fulvic acids. J. Hazard Mater. 279, 569–578.

Fendorf, S., Michael, H.A., van Geen, A., 2010. Spatial and temporal variations of groundwater arsenic in South and Southeast Asia. Science 328 (5982), 1123–1127.

Hoffmann, M., Mikutta, C., Kretzschmar, R., 2012. Bisulfide reaction with natural organic matter enhances arsenite sorption: insights from X-ray absorption spectroscopy. Environ. Sci. Technol. 46 (21), 11788–11797.

Hoffmann, M., Mikutta, C., Kretzschmar, R., 2013. Arsenite binding to natural organic matter: spectroscopic evidence for ligand exchange and ternary complex formation. Environ. Sci. Technol. 47 (21), 12165–12173.

Joe-Wong, C., Shoenfelt, E., Hauser, E.J., Crompton, N., Myneni, S.C., 2012. Estimation of reactive thiol concentrations in dissolved organic matter and bacterial cell membranes in aquatic systems. Environ. Sci. Technol. 46 (18), 9854–9861.

Jomova, K., Jenisova, Z., Feszterova, M., Baros, S., Liska, J., Hudecova, D., Rhodes, C., Valko, M., 2011. Arsenic: toxicity, oxidative stress and human disease. J. Appl. Toxicol. 31 (2), 95–107.

Kwasniewski, M.T., Allison, R.B., Wilcox, W.F., Sacks, G.L., 2011. Convenient, inexpensive quantification of elemental sulfur by simultaneous in situ reduction and colorimetric detection. Anal. Chim. Acta 703 (1), 52–57.

Langner, P., Mikutta, C., Kretzschmar, R., 2012. Arsenic sequestration by organic sulphur in peat. Nat. Geosci. 5 (1), 66–73.

Langner, P., Mikutta, C., Suess, E., Marcus, M.A., Kretzschmar, R., 2013. Spatial distribution and speciation of arsenic in peat studied with microfocused X-ray fluorescence spectrometry and X-ray absorption spectroscopy. Environ. Sci. Technol. 47 (17), 9706–9714.

Lenoble, V., Dang, D., Cazalet, M.L., Mounier, S., Pfeifer, H.-R., Garnier, C., 2015. Evaluation and modelling of dissolved organic matter reactivity toward AsIII and AsV–Implication in environmental arsenic speciation. Talanta 134, 530–537.

Li, G., Sun, G.-X., Williams, P.N., Nunes, L., Zhu, Y.-G., 2011. Inorganic arsenic in Chinese food and its cancer risk. Environ. Int. 37 (7), 1219–1225.

Lin, T.Y., Hafeznezami, S., Rice, L., Lee, J., Maki, A., Sevilla, T., Stahl, M., Neumann, R., Harvey, C., Suffet, I.M., 2017. Arsenic oxyanion binding to NOM from dung and aquaculture pond sediments in Bangladesh: importance of site-specific binding constants. Appl. Geochem. 78, 234–240.

Liu, G., Cai, Y., 2010. Complexation of arsenite with dissolved organic matter: conditional distribution coefficients and apparent stability constants. Chemosphere 81 (7), 890–896.

Liu, G., Cai, Y., 2013. Studying arsenite–humic acid complexation using size exclusion chromatography–inductively coupled plasma mass spectrometry. J. Hazard Mater. 262, 1223–1229.

Liu, G., Fernandez, A., Cai, Y., 2011. Complexation of arsenite with humic acid in the presence of ferric iron. Environ. Sci. Technol. 45 (8), 3210–3216.

Ma, H., Allen, H.E., Yin, Y., 2001. Characterization of isolated fractions of dissolved organic matter from natural waters and a wastewater effluent. Water Res. 35 (4), 985–996.

Maguffin, S.C., Abu-Ali, L., Tappero, R.V., Pena, J., Rohila, J.S., McClung, A.M., Reid, M. C., 2020. Influence of manganese abundances on iron and arsenic solubility in rice paddy soils. Geochem. Cosmochim. Acta 276, 50–69.

Meng, Y.-L., Liu, Z., Rosen, B.P., 2004. As (III) and Sb (III) uptake by GlpF and efflux by ArsB in Escherichia coli. J. Biol. Chem. 279 (18), 18334–18341.

Mikutta, C., Kretzschmar, R., 2011. Spectroscopic evidence for ternary complex formation between arsenate and ferric iron complexes of humic substances. Environ. Sci. Technol. 45 (22), 9550–9557.

Pothier, M.P., Hinz, A.J., Poulain, A.J., 2018. Insights into arsenite and arsenate uptake pathways using a whole cell biosensor. Front. Microbiol. 9, 2310.

Pothier, M.P., Lenoble, V., Garnier, C., Misson, B., Rentmeister, C., Poulain, A.J., 2020. Dissolved organic matter controls of arsenic bioavailability to bacteria. Sci. Total Environ. 716, 137118.

Qian, G., Xu, L., Li, N., Wang, K., Qu, Y., Xu, Y., 2022. Enhanced arsenic migration in tailings soil with the addition of humic acid, fulvic acid and thiol-modified humic acid. Chemosphere 286, 131784.

RCore, T.R., 2013. A Language and Environment for Statistical Computing. R Foundation for Statistical Computing, Vienna, Austria. *Online:*. http://www.R-project.org.

Redman, A.D., Macalady, D.L., Ahmann, D., 2002. Natural organic matter affects arsenic speciation and sorption onto hematite. Environ. Sci. Technol. 36 (13), 2889–2896.

Reid, M.C., Maillard, J., Bagnoud, A., Falquet, L., Le Vo, P., Bernier-Latmani, R., 2017. Arsenic methylation dynamics in a rice paddy soil anaerobic enrichment culture. Environ. Sci. Technol. 51 (18), 10546–10554.

Ren, J., Fan, W., Wang, X., Ma, Q., Li, X., Xu, Z., Wei, C., 2017. Influences of size-fractionated humic acids on arsenite and arsenate complexation and toxicity to Daphnia magna. Water Res. 108, 68–77.
Roberts, L.C., Hug, S.J., Voegelin, A., Dittmar, J., Kretzschmar, R., Wehrli, B., Saha, G.C., Badruzzaman, A.B.M., Ali, M.A., 2011. Arsenic dynamics in porewater of an intermittently irrigated paddy field in Bangladesh. Environ. Sci. Technol. 45 (3), 971–976.
Rosen, B.P., Liu, Z., 2009. Transport pathways for arsenic and selenium: a minireview. Environ. Int. 35 (3), 512–515.
Sharma, P., Ofner, J., Kappler, A., 2010. Formation of binary and ternary colloids and dissolved complexes of organic matter, Fe and as. Environ. Sci. Technol. 44 (12), 4479–4485.
Skyllberg, U., Qian, J., Frech, W., 2005. Combined XANES and EXAFS study on the bonding of methyl mercury to thiol groups in soil and aquatic organic matter. Phys. Scripta 2005 (T115), 894.
Slyemi, D., Bonnefoy, V., 2012. How prokaryotes deal with arsenic. Environ. Microbiol. Rep. 4 (6), 571–586.
Smedley, P.L., Kinniburgh, D.G., 2002. A review of the source, behaviour and distribution of arsenic in natural waters. Appl. Geochem. 17 (5), 517–568.
Song, W.Y., et al., 2010. Arsenic tolerance in Arabidopsis is mediated by two ABCC-type phytochelatin transporters. Proc. Natl. Acad. Sci. U.S.A. 107 (49), 21187–21192.
Spuches, A.M., Kruszyna, H.G., Rich, A.M., Wilcox, D.E., 2005. Thermodynamics of the as (III)− thiol interaction: arsenite and monomethylarsenite complexes with glutathione, dihydrolipoic acid, and other thiol ligands. Inorg. Chem. 44 (8), 2964–2972.
Stocker, J., Balluch, D., Gsell, M., Harms, H., Feliciano, J., Daunert, S., Malik, K.A., Van der Meer, J.R., 2003. Development of a set of simple bacterial biosensors for quantitative and rapid measurements of arsenite and arsenate in potable water. Environ. Sci. Technol. 37 (20), 4743–4750.
Stookey, L.L., 1970. Ferrozine—a new spectrophotometric reagent for iron. Anal. Chem. 42 (7), 779–781.
Viacava, K., Qiao, J., Janowczyk, A., Poudel, S., Jacquemin, N., Meibom, K.L., Shrestha, H.K., Reid, M.C., Hettich, R.L., Bernier-Latmani, R., 2022. Meta-omics-aided isolation of an elusive anaerobic arsenic-methylating soil bacterium. ISME J. 1–10.
Wang, J., Kerl, C.F., Hu, P., Martin, M., Mu, T., Brüggenwirth, L., Wu, G., Said-Pullicino, D., Romani, M., Wu, L., 2020. Thiolated arsenic species observed in rice paddy pore waters. Nat. Geosci. 13 (4), 282–287.
Warwick, P., Inam, E., Evans, N., 2005. Arsenic's interaction with humic acid. Environ. Chem. 2 (2), 119–124.
Xu, Y., Wang, K., Zhou, Q., Zhang, L., Qian, G., 2020. Effects of humus on the mobility of arsenic in tailing soil and the thiol-modification of humus. Chemosphere 259, 127403.
Yao, Y., Mi, N., He, C., Yin, L., Zhou, D., Zhang, Y., Sun, H., Yang, S., Li, S., He, H., 2020. Transport of arsenic loaded by ferric humate colloid in saturated porous media. Chemosphere 240, 124987.
Zhang, X., Reid, M.C., 2022. Inhibition of methanogenesis leads to accumulation of methylated arsenic species and enhances arsenic volatilization from rice paddy soil. Sci. Total Environ. 818, 151696.
Zhao, F., Ma, J., Meharg, A., McGrath, S., 2009. Arsenic uptake and metabolism in plants. New Phytol. 181 (4), 777–794.
Zhu, Y.-G., Yoshinaga, M., Zhao, F.-J., Rosen, B.P., 2014. Earth abides arsenic biotransformations. Annu. Rev. Earth Planet Sci. 42, 443.